

Provided for non-commercial research and education use.  
Not for reproduction, distribution or commercial use.



This article appeared in a journal published by Elsevier. The attached copy is furnished to the author for internal non-commercial research and education use, including for instruction at the authors institution and sharing with colleagues.

Other uses, including reproduction and distribution, or selling or licensing copies, or posting to personal, institutional or third party websites are prohibited.

In most cases authors are permitted to post their version of the article (e.g. in Word or Tex form) to their personal website or institutional repository. Authors requiring further information regarding Elsevier's archiving and manuscript policies are encouraged to visit:

<http://www.elsevier.com/copyright>



Contents lists available at ScienceDirect

## Vision Research

journal homepage: [www.elsevier.com/locate/visres](http://www.elsevier.com/locate/visres)Relative mislocalization of successively presented stimuli<sup>☆</sup>Diana Bocianski<sup>a,\*</sup>, Jochen Müsseler<sup>a</sup>, Wolfram Erlhagen<sup>b</sup><sup>a</sup>Psychology Department, RWTH Aachen University, Jägerstrasse 17-19, 52066 Aachen, Germany<sup>b</sup>Department of Mathematics for Science and Technology, University of Minho, Portugal

## ARTICLE INFO

## Article history:

Received 19 February 2008

Received in revised form 27 May 2008

## Keywords:

Localization error

Relative judgment

Space perception

Visual illusion

Spatial cuing

## ABSTRACT

When observers were asked to localize the peripheral position of a briefly presented target with respect to a previously presented comparison stimulus, they tended to judge the target as being more towards the fovea than the comparison stimulus. Three experiments revealed that the mislocalization only emerged when the comparison stimulus and the target were presented successively. Varying the temporal interval between stimuli showed that the mislocalization reversed with longer stimulus-onset asynchronies. Further, the mislocalization was increased with a decrease of the spatial distance between stimuli. These findings suggested that the mislocalization originated from local excitatory and inhibitory mechanisms. Corroborating this idea a neuronal dynamic field model was successfully developed to account for the findings.

© 2008 Elsevier Ltd. All rights reserved.

## 1. Relative mislocalization of successively presented stimuli

Typically, the visual system processes the position of targets with high precision—at least when these targets are presented stationary with high contrast and without time restrictions so that observers can easily fixate them. Localization is much poorer or is even distorted when targets are briefly presented before, during or after a saccade or during smooth pursuit eye movements (e.g., Awater & Lappe, 2006; Brenner, Smeets, & van den Berg, 2001; Rotman, Brenner, & Smeets, 2005).

However, there are also studies reporting distortions with briefly presented stimuli during steady eye fixation. In some of these studies, (involuntary) microsaccades towards the stimuli were observed which seemed to affect their perceived positions (e.g., Fahle, 1991; Findlay, 1974; Matin, Pola, Matin, & Picoult, 1981). The distortions were gathered with absolute and relative localization tasks. In studies with absolute localization tasks observers pointed with their finger or with a computer mouse to the targets' location. For example, in a study of Sheth and Shimojo (2001) targets were briefly presented in peripheral space. After a short delay following the targets' disappearance, observers locate the target position by means of a computer mouse. Mislocalizations emerged systematically toward the center of the gaze (foveal mislocalization, see also Kerzel, 2002; Müsseler & Aschersleben,

<sup>☆</sup> We thank the anonymous reviewers for helpful comments and suggestions and Thomas Klapdor and Stefan Ladwig for carrying out the experiments. This research was supported by a grant from the Deutsche Forschungsgemeinschaft to the second author (DFG MU 1298/4) and a grant from the Acções Integradas Luso-Alemãs to the third author (Acção No A-12/06).

\* Corresponding author. Fax: +49 241 80 92318.

E-mail address: [diana.bocianski@psych.rwth-aachen.de](mailto:diana.bocianski@psych.rwth-aachen.de) (D. Bocianski).

1998; Müsseler, van der Heijden, Mahmud, Deubel, & Ertsey, 1999; O'Regan, 1984; van der Heijden, Müsseler, & Bridgeman, 1999a). Additionally, mislocalizations were in direction of salient markers in the visual display. A perceptual judgment task revealed that the localization error is independent from the execution of eye movements. The amplitude of distortion enhanced with an increasing time interval between targets disappearance and judgment. Thus, this compression phenomenon seemed to establish a visual memory effect according to which the spatial location is systematically distorted over time.

Uddin, Kawabe and Nakamizo (2005) investigated the influence of spatial and temporal factors on localization of visual stationary targets. Spatial variation consisted in display manipulation with or without distractors. Target and distractor were presented either simultaneously, for 150 or 1000 ms while observers had to memorize the targets position under fixed gaze conditions. 150 ms after stimuli offset a mouse cursor was shown to adjust the remembered target position. Under the condition of 150 ms presentation time and distractor presence, judgment performance remained unbiased, whereas with 1000 ms presentation time and distractor presence as well as absence, a foveal bias was observed.

In relative localization tasks observers judged the targets' position with regard to the location of a comparison stimulus (e.g., Foley, 1976; Kerzel, 2002). For example, Kerzel (2002) examined the influence of foveal mislocalization and memory averaging on memory for the position of stationary objects, presented briefly in the periphery. When a distractor was flashed during the retention interval after targets presentation and even when the distractor was visible throughout the trial, a bias away from the distractor was observed. However, a foveal tendency existed regardless of additional presented objects.

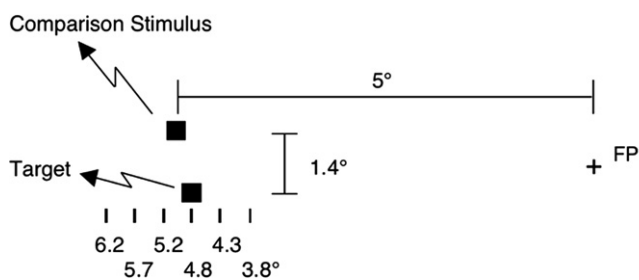


**Fig. 1.** Stimulus presentation in the experiments. Participants fixated a cross in the middle of a screen. A stimulus configuration consisting of an upper square (comparison stimulus) and a lower square (target) appeared to the left or to the right of the fixation cross (here 5° to the left). Participants' task was to judge whether the target (presented at 3.8°–6.2°) or the comparison stimulus was perceived more outer.

Using also a relative judgment task, an incidental observation of Müsseler and co-workers (Müsseler et al., 1999, Exp. 5) revealed a related localization error. In one of their conditions the authors asked observers to localize the peripheral position of a single target with respect to a comparison stimulus presented above the target (Fig. 1). Both stimuli were briefly flashed with the comparison first, followed by the target with a stimulus onset asynchrony (SOA) of about 100 ms. The authors found with these presentation conditions that observers tended to judge the target as being more towards the fovea than the comparison stimulus (or the comparison stimulus as being more peripheral than the target, respectively).

For a first rough explanation of this mislocalization, the authors referred to the method of constant stimuli, which was applied in their study. The comparison stimulus was presented at a fixed position, whereas the target was presented below with constant eccentricities varying between 3.8° and 6.8°. Observers' task was always to judge whether the upper or the lower stimulus was more peripheral (which implies that the other stimulus was perceived more foveal). The authors assumed that the explanation of the relative mislocalization was in the varying eccentricities of the targets. Adding the reasonable assumption that localization judgments became more variable with eccentricity, the distributions of perceived target positions were presumed to get flatter the more the target's eccentricity is. From that, it simply followed that the overall distribution of judgments had a skewness towards more foveal judgments. In the following we will refer to this explanation as the variability-by-eccentricity assumption. Note, that according to this explanation the mislocalization was not a perceptual phenomenon, which can be 'perceived' in a single trial. Instead the mislocalization emerges only from the distribution of judgments over trials, which were affected by the different targets' eccentricities.

In the present paper we started with the variability-by-eccentricity assumption, which remained unchallenged so far. Experiments 1 aimed to replicate the mislocalization and to examine specific hypotheses derived from the variability-by-eccentricity assumption. In Experiments 2 and 3 the spatial and temporal distance between stimuli was varied to examine whether local excitatory or inhibitory mechanisms contribute to the mislocalization.

## 2. Experiment 1

In the study of Müsseler and co-workers (1999, Exp. 5) the comparison stimulus was always presented first, followed by the target presented below at varying eccentricities. In the present experiment we examined whether the localization error occurred also

when the temporal sequence between stimuli was reversed. If it would always be the second stimulus, which is localized more towards the fovea, the mislocalization is expected to reverse too. In other words, the comparison stimulus in Fig. 1 should be judged more foveal. Contrary, nothing essential would be changed when considering the variability-by-eccentricity assumption. The lower target's positions were still varying, what should result in more inner judgments of the lower stimulus, i.e., in this case of the first stimulus (i.e., the target in Fig. 1).

Therefore, in the present experiment stimuli were presented with a positive (the comparison stimulus comes first) and a negative SOA (the target comes first). Additionally, both stimuli were presented simultaneously. In this case, it can be assumed that they were processed as one stimulus with veridical relative position information. With simultaneous presentation we expect that relative position judgments are more or less error-free (see also Müsseler & van der Heijden, 2004).

### 2.1. Method

#### 2.1.1. Apparatus and stimuli

The experiments were carried out in a dimly lit and soundproof chamber and were controlled by an Apple Macintosh computer with Matlab software using the Psychophysics Toolbox extension (Brainard, 1997; Pelli, 1997). The stimuli were presented on a 22" color CRT monitor (Iiyama Vision Master Pro 513, 100 Hz refresh rate, 1024 × 768 pix). The observers sat at a table with a chin rest and were positioned at a viewing distance of 50 cm to the display.

The stimuli were made up of two singular dark squares (1.9 cd/m<sup>2</sup>) on a light background (68 cd/m<sup>2</sup>) and had a size of 0.33° × 0.33°, respectively. The display consisted of a single upper square (the comparison stimulus) and a single lower square (the target). The position of the comparison stimulus was held constant at 5° in the left or right visual field. The probe's position had a vertical distance of 1.4° to the comparison stimulus and was horizontally varied with respect to the mid-position of the comparison stimulus by ±0.2°, ±0.7°, and ±1.2°; thus, the target was presented at 3.8°, 4.3°, 4.8°, 5.2°, 5.7°, or 6.2°.

#### 2.1.2. Design

Target and comparison stimulus were presented unpredictably in either the left or the right visual field. They appeared either simultaneously or the target followed the comparison stimulus by an SOA of +100 ms or the sequence of presentation was reversed (SOA of −100 ms). Each combination of hemifield (left vs. right) × SOA (+100, 0, −100 ms) × probe position (3.8–6.2°) was presented to all participants in two blocks. In one block the SOAs of 0 and −100 ms were randomly combined with the target positions, in the other block the SOAs of 0 and +100 ms are applied. The sequence of blocks was counterbalanced between participants.

#### 2.1.3. Procedure

The fixation cross was visible throughout the experiment and the instruction stressed concentration on the fixation point. The participants initiated stimulus presentation by pressing a mouse button. Three hundred milliseconds after a beep the target and the comparison stimulus were presented. The participants were asked to judge whether the upper square (comparison stimulus) or the lower square (target) was perceived as being more peripheral; accordingly they pressed the upper button of a horizontally arranged mouse for the upper square and the lower button for the lower square. Following a response, the next trial was triggered after 1 s. A training period of 48 trials and the experimental session of 2 × 288 trials lasted about 30 min.

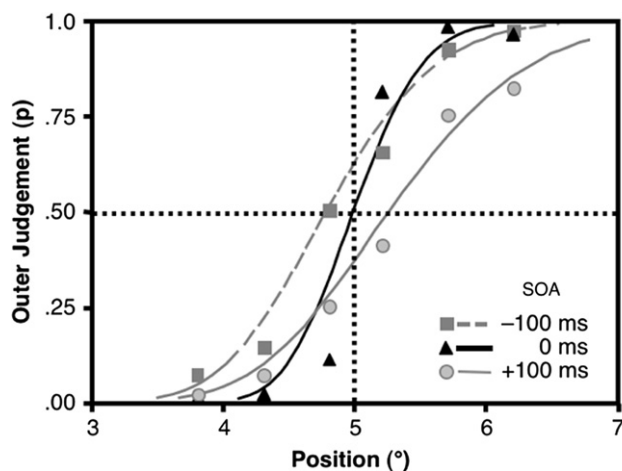


**Fig. 2.** Mean probabilities of outer judgments of the target and fitted functions for the three stimulus-onset asynchronies (SOAs) between comparison stimulus and target (−100, 0, and +100 ms). A more eccentric deviation of the function from the objective mid-position (5°) means that the point of subjective equality is more peripheral thus the target is perceived more towards the fovea and vice versa (Experiment 1,  $N = 10$ ).

#### 2.1.4. Participants

Ten individuals (7 females) with a mean age of 27.0 years were paid to participate in the experiment. All participants in the present and the subsequent experiments reported having normal or corrected-to-normal vision.

#### 2.2. Results

For every participant and condition the frequency of trials were counted in which the target was perceived more outer than the comparison stimulus. Frequencies of the judgments at the six target positions were entered in a Probit analysis of the Psignifit Software Package, which determined the 50%-threshold points of subjective equality (PSE) for every participant and condition (bootstrap-software.org, cf. Wichmann & Hill, 2001a; Wichmann & Hill, 2001b). Positive deviations indicate PSE values higher than the objective mid-position and thus a tendency to more inner judgments of the target (Fig. 2).

The PSE values were dependent variables in a 2 (left vs. right hemifield)  $\times$  3 (SOAs of −100, 0, and +100 ms) analysis of variance (ANOVA). The analysis revealed no effect of the hemifield and the interaction (both  $p$ 's  $> .20$ ), but a significance of the SOA factor with  $F(9, 18) = 8.91$ ,  $MSE = 74.75$ ,  $p = .009$ <sup>1</sup>. When the comparison stimulus was presented first (SOA = +100 ms), participants judged it as being more outer than the target; or the other way around, they judged the target as being more inner than the comparison stimulus (mean PSE deviation from the objective mid-position of 0.33°). When the target was presented first (SOA = −100 ms), participants judged the comparison stimulus as being more inner than the target (mean PSE deviation of −0.20°). With simultaneously presented stimuli, localization judgments were nearly error free (PSE deviation of 0.03°). Correspondingly,  $t$ -tests yielded (nearly) significant differences between the SOA conditions of −100 and 0 ms [ $t(9) = 2.19$ ,  $p = .057$ ] and between 0 and +100 ms [ $t(9) = -3.16$ ,  $p = .011$ ; two-tailed].

<sup>1</sup> In order to avoid the risk of violating statistical assumptions that is present in repeated-measures designs due to inhomogeneity of the variance-covariance matrix,  $F$ -probabilities in the present and the following experiments were corrected according to Huynh and Feldt (1980).

#### 2.3. Discussion

Four main results were observed. The first finding was that localization judgments were not affected by the left/right visual field, in which the stimuli appeared. In the subsequent experiments we will therefore average across this factor.

The second finding was that relative judgments were nearly error free when the two stimuli were presented simultaneously. We take that as evidence that in this case stimuli were processed as one stimulus with veridical relative position information between them (cf. Müsseler & van der Heijden, 2004; van der Heijden et al., 1999a).

The third finding was that mislocalizations emerged when both stimuli are presented successively. When the comparison stimulus (the upper stimulus) was presented first, we observed a deviation of the PSE value from the objective mid-position of 0.33°. This value matches nearly with the PSE deviation of 0.43°, which was observed under similar conditions in the predecessor's study (Müsseler et al., 1999, Exp. 5). Thus, we successfully replicated the reported mislocalization.

The fourth and main finding was that the mislocalization was reversed when the sequence of stimulus presentation is reversed. Or in other words, it was always the second stimulus, which was judged as the more inner stimulus. This finding was not in accordance with our variability-by-eccentricity explanation of the mislocalization. With regard to this explanation the mislocalization should originate from the method of constant stimuli only, more precisely from the different target eccentricities across trials. However, in both SOA conditions, the lower target's positions were still varying in eccentricity, what should result in more inner judgments of the lower stimulus independently from the temporal sequence of presentation, but it was. Instead, the finding can be taken as first evidence that the mislocalization originated from perceptual mechanisms and not from the method used. In the subsequent experiments we examined whether the mislocalization was sensitive for spatio-temporal variations.

#### 3. Experiment 2

The main finding of Experiment 1, which indicated that the mislocalization was reversed when the temporal sequence of stimulus presentation was reversed, pointed to a spatio-temporal explanation. For example, it is possible to think of an interpretation of the mislocalization based upon the idea that briefly presented stimuli are first localized more foveally and than "move outwards" over time. Then, when the target is displayed, the previously presented comparison stimulus could already have "moved" more outwards. In this case, the mislocalization should be reversed with the reversal of presentation—as it was. What needs to be specified is, of course, the mechanism, which causes moving-outward movements over time.

Several recent studies identified locally working mechanisms according to which the presentation of a stimulus elicits excitatory and inhibitory processes determining a temporal activation pattern, which is not restricted to the area covered by the stimulus. Rather it spreads its activation to and integrates contextual information from the adjacent parts of the visual field (e.g., Berry, Brivanlou, Jordan, & Meister, 1999; Erlhagen & Jancke, 2004; Kirschfeld & Kammer, 1999; Müsseler & van der Heijden, 2004). To examine whether the present mislocalization was caused by such a mechanism, the temporal interval between stimuli was varied in the present experiment. In the previous experiment, stimuli were presented only with the 0-ms and the 100-ms SOA. Comparison stimulus and target were now temporarily separated by seven SOAs varying between 0 and 700 ms.

### 3.1. Method

#### 3.1.1. Stimuli, design and procedure

These were essentially the same as in Experiment 1 with the following changes. Seven SOAs between comparison stimulus and target were introduced: 0, 50, 150, 250, 350, 500 or 700 ms. Each combination of hemifield (left vs. right visual field)  $\times$  target positions ( $3.8^\circ$ – $6.2^\circ$ )  $\times$  SOAs was presented to all participants in a randomized sequence. A training period of 48 trials and the experimental session of 8 blocks—each with 84 trials—lasted about 45 min.

#### 3.1.2. Control of eye fixation

In the previous experiment the presentation of comparison stimulus and target was much too short to execute eye movements successfully. Additionally, keeping fixation seems to be much more convenient for the observers than moving their eyes. However, in the present experiment eye movements were more critical to occur especially with the SOAs of 500 and 700 ms. Therefore, the horizontal position of the right eye was monitored with a head mounted and infrared light reflecting eye-tracking device (Skalar Medical B.V., IRIS Model 6500). A horizontal three point calibration was made at the beginning of each block. If a saccade was detected during the presentation of the target stimulus, the data of the corresponding trial was excluded from analysis. The mean exclusion rate was only 1.26%, overall 127 of 10,080 trials.

#### 3.1.3. Participants

Fifteen individuals with a mean age of 27.0 years were paid to participate in the experiment.

### 3.2. Results and discussion

Again, the PSE-values were computed for every participant and condition. Fig. 3 shows the mean PSE-values of the seven SOAs (solid line). With a simultaneous presentation of comparison stimulus and target, the observed PSE value of  $0.05^\circ$  replicated the nearly error-free localizations of the previous experiments. With an increase of the SOA, positive localization errors (i.e., the target is perceived more inner) reached a maximum at the SOAs of 150 and 250 ms and then decreased again (PSE values with the 50, 150, 250 and 350-ms SOA:  $0.09^\circ$ ,  $0.19^\circ$ ,  $0.15^\circ$ , and  $0.06^\circ$ , respectively). The localization error was even reversed with the SOAs of

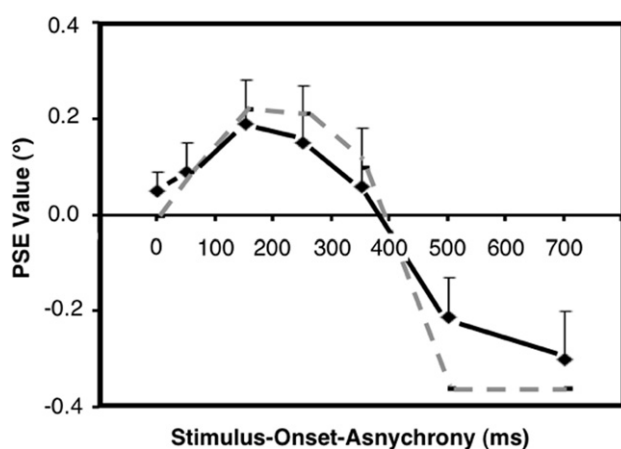


**Fig. 3.** Mean points of subjective equality (PSE) and standard errors between participants for the seven SOAs between comparison stimulus and target (solid line, Experiment 2,  $N = 15$ ). The data points of the dashed line were derived from a dynamic field model, which depicts the relative peak positions associated with the target at a fixed activation level for all SOAs (see Section 5).

500 ms ( $-0.21^\circ$ ) and 700 ms ( $-0.30^\circ$ ). An one-way ANOVA with repeated measurements yielded a significant SOA effect with  $F(6,84) = 9.00$ ,  $MSE = 28.50$ ,  $p < .001$ .

The findings indicated that local mechanisms contributed to or even were at the basis of the observed mislocalization. The characteristic trend with an initial increase of the localization error in a first phase (up to 250-ms SOA) and an adjacent decrease with a reversion of the localization error (with the 500 and 700-ms SOA) could be taken as evidence for local interactions of excitatory and inhibitory mechanisms over time. In Section 5, a dynamic field model is proposed which specify and test the underlying mechanisms of the trend in more detail.

It is striking to note that the point of inflection from positive to negative localization error corresponded roughly with the point in time at which priming mechanisms are known to turn into inhibition mechanism: Speeded reaction times in response to a target are known to be facilitated when a peripheral cue preceded the target by about 100–300 ms. However, it is also known from the inhibition-of-return phenomenon (IOR) that the facilitation turns into a disadvantage when the target is presented afterwards (for perhaps 500–2000 ms after the cue; e.g., Klein, 2000; Posner & Cohen, 1984). It has been speculated that IOR promotes exploration of new, previously unattended objects in the scene by preventing attention from returning to already-attended objects. Despite the comparable time courses it is not clear whether IOR in reaction times is related somehow to the present localization error. One problem is that information about object localization is rarely gathered in priming paradigms so far (but see Hagenaar & van der Heijden, 1997; van der Heijden, van der Geest, De Leeuw, Krikke, & Müsseler, 1999b).

## 4. Experiment 3

If spatial interactions of local excitatory and inhibitory processes contribute to or were even at the basis of the localization error, the effect should be increased with nearby presented stimuli and should be decreased with far-away presented stimuli. Therefore the vertical inter-stimulus distance was varied in the present experiment.

### 4.1. Method

#### 4.1.1. Stimuli, design and procedure

These were essentially the same as in Experiment 1 with the following changes. Target and comparison stimulus were presented with a vertical spatial distance from the horizontal meridian through the fixation cross of 0.35, 0.70, 1.05, 2.1 or  $2.8^\circ$ . Thus, their total spatial distance was 0.7, 1.4, 2.1, 4.2, or  $5.6^\circ$ . Vertical inter-stimulus distances were presented blockwise with the sequence of blocks counterbalanced between participants. As in the previous experiments, targets' horizontal positions ( $3.8^\circ$ – $6.2^\circ$ ) and SOAs (0 and +100 ms) were randomized within a block. After a training phase of 48 trials observers passed through the five blocks with 96 trials each.

#### 4.1.2. Participants

Fourteen individuals with a mean age of 23.0 years were paid to participate in the experiment.

### 4.2. Results and discussion

Fig. 4 shows the mean PSE-values for the five vertical distances. The solid line depicts PSE-values of the 100-ms SOA condition: When the vertical distance between stimuli was increased from 0.7, 1.4, 2.1, 4.2, to  $5.6^\circ$ , the mean PSE values decreased from by

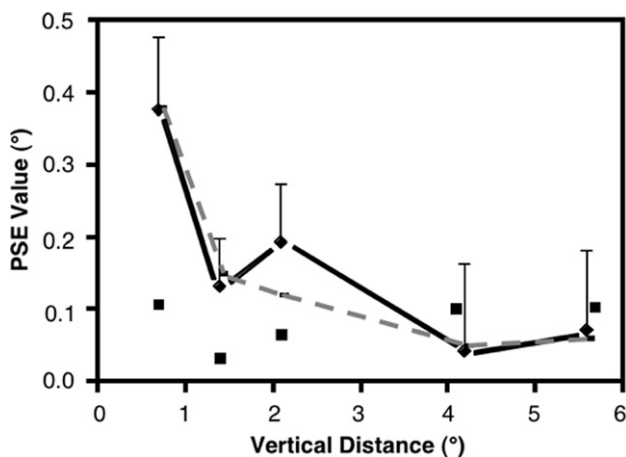


**Fig. 4.** Mean points of subjective equality (PSE) for the five vertical distances between comparison stimulus and target. The solid line depicts PSE-values with 100-ms SOA; squares represent PSE-values with the 0-ms SOA (Experiment 3,  $N = 14$ ). The data points of the dashed line were obtained from the dynamic field model (see Section 5).

0.38, 0.13, 0.19, 0.04, to 0.07°. PSE-values were nearly parallel to the abscissa in the 0-ms SOA condition (squares) with a mean deviation of 0.08°. Accordingly, a 5 (vertical distance)  $\times$  2 (SOA) ANOVA revealed a significant interaction of both factors [ $F(4,52) = 3.48$ ,  $MSE = 0.04$ ,  $p = .027$ ] and a tendency for a main effect of vertical distance,  $F(4,52) = 2.35$ ,  $MSE = 0.06$ ,  $p = .088$ .

The observation that the mislocalization was increased when the distance between stimuli was decreased is clear evidence that local mechanisms contributed to the mislocalization. In the subsequent section, a dynamic field model specifies possible locally working mechanisms.

## 5. General discussion

In three experiments we examined a localization error, which was observed when a briefly presented target appeared in the retinal periphery and observers' task was to judge its position relatively to a previously presented comparison stimulus. Experiment 1 replicated and extended the basic observation that with these conditions observers judged the target as being more towards the fovea than the comparison stimulus (cf. Müseler et al., 1999, Exp. 5). The mislocalization was observed only when both stimuli were presented successively. Moreover, when the sequence of stimulus presentations was reversed, results showed that it was always the second stimulus, which was judged as the more inner stimulus. The temporal interval between stimuli was varied in Experiment 2. Most interestingly, the localization error increased in a first phase (up to the 250-ms SOA) and then decreased in an adjacent phase leading to a reversion of the effect (with the 500- and 700-ms SOA). The results of Experiment 3 demonstrated that the mislocalization increased with small inter-stimulus distances.

The findings of the experiments ruled out the variability-by-eccentricity assumption according to which the mislocalization emerged from the varying target eccentricities necessary to apply the method of constant stimuli. In all experiments the lower target's positions were always varying in eccentricity, what should result in more inner judgments of the lower stimulus independently from the factorial variations in the experiments, but they were.

Instead, the dynamic trends in the data let us speculate that the localization error originated from locally working interactions of excitatory and inhibitory mechanisms. To specify this hypothesis we applied a dynamic field model to the data, which is described

in the subsequent section. In particular we were interested to understand the reversal of the error with sufficiently large SOAs (Exp. 2) and then try to apply the model to the distance variation (Exp. 3).

It is worth to note that the model has been originally developed to explain nonlinear interaction effects observed in neural populations of primary visual cortex (Jancke et al., 1999). Later, the model was extended to discuss potential neural correlates of systematic misperceptions of the position of a moving object known as the Fröhlich effect, the representational momentum and the flash-lag illusion (Erlhagen, 2003; Erlhagen & Jancke, 2004; Jancke & Erlhagen, 2008; see also Müseler, Stork, & Kerzel, 2002).

## 6. A dynamic field model accounting for the localization error

The dynamic field model implements the idea that the information about the horizontal position is represented by the dynamic activity pattern of local populations of interconnected spatially tuned neurons. The population response is triggered by afferent input carrying the retinal information and shaped by interactions within the neural ensemble. Since the neurons split into an excitatory and an inhibitory subpopulation, the evolving activity pattern in response to a brief input of adequate intensity is transient in nature (Wilson & Cowan, 1973). Recurrent excitatory interactions lead to a continuous increase of the activation level event after stimulus offset. The inhibitory population spatially integrates this activity and feeds back locally to the excitatory population. As a result, the population activity reaches a peak value when the excitation is counterbalance by the inhibition, and then decays back to resting level. The interactions depend on the functional distance of the field elements, with excitatory coupling between neurons with similar preferred position and inhibition dominating for larger distances. This functional circuitry, known as Mexican-hat organization, guarantees that the transient population response remains localized in position space.

To account for the relative localization errors observed in the experiments we made two main adjustments to the basic field model used in our previous work (for details of the mathematical model see the Appendix). First, we adapted the time scale of the equations describing the population dynamics to reflect the experimentally observed temporal interaction effects, which span several hundred milliseconds (SOAs varying between 0 and 700-ms in Exp. 2). A second modification concerns the spatial interactions. Fig. 5A depicts the Gaussian weight profiles for the integration within the excitatory population (solid line) and for the integration from the excitatory to the inhibitory population (dashed line) that we used for the model simulations. The profiles are not symmetric (e.g., reciprocal connections are not equal) but shifted to some extent in the direction of the fovea. This means that a neuron tuned to position  $x^\circ$  does not get its strongest input from the direct field neighbor but from a neuron with a preferred position  $(x - \Delta x)^\circ$  closer to the fovea. As can be clearly seen in Fig. 5B, this bias causes the population activity,  $u(x)$ , to drift in the direction of the fovea. The magnitude of the shift  $\Delta x$  determines the magnitude of the drift. This model parameter was calibrated to account for the systematic mislocalization of a stimulus flashed at 5° in the periphery. As found in absolute judgment tasks, the magnitude of the localization error is about 10% of targets' eccentricity, thus estimating in our case 0.5° (van der Heijden et al., 1999b; van der Heijden et al., 1999a).

The model explains the observed spatiotemporal interaction effect as the result of an integration of sub-threshold activation induced by the vertically displaced stimuli. There is a large body of experimental evidence showing that stimuli presented outside the classical receptive field (the region of visual space in which

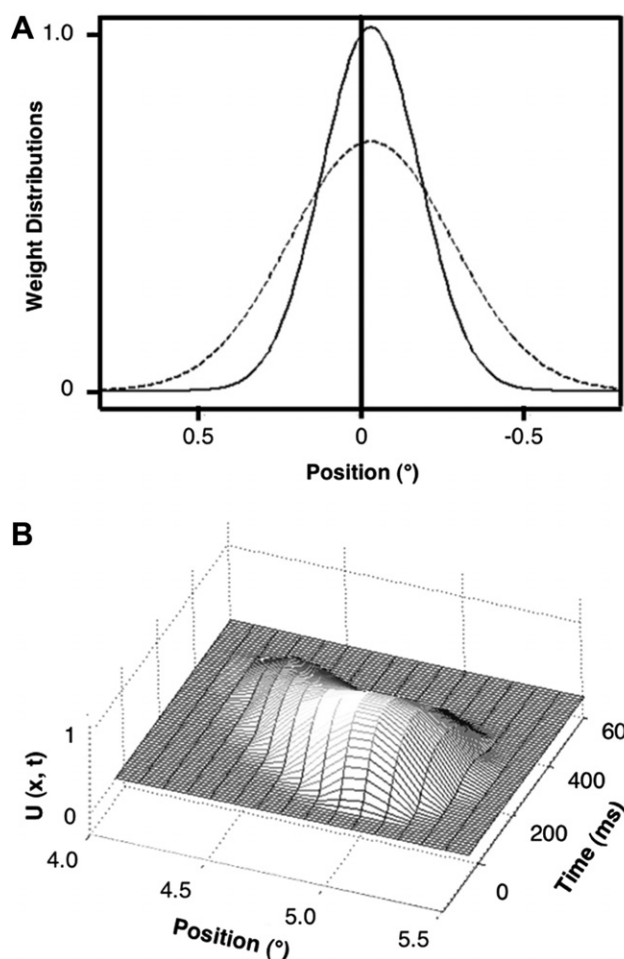


**Fig. 5.** (A) Gaussian weight profiles for the spatial integration of activity within the excitatory population (solid line) and from the excitatory to the inhibitory population (dashed line) are shown. The profiles are slightly shifted in the direction of the fovea. (B) The spatiotemporal evolution of the normalized response of the excitatory population,  $u(x,t)$ , to a briefly flashed afferent stimulus at  $x = 5^\circ$  is shown. Note the drift of the peak position in the direction of the fixation point ( $x = 0^\circ$ ).

stimuli evoke spike discharge) can facilitate or suppress supra-threshold responses of cells in visual cortex. Long-range horizontal connections are thought to constitute a neural substrate for spreading sub-threshold activity (for a review see Fitzpatrick, 2000). The potential impact on the perceptual level has been directly investigated in a recent experiment by Jancke, Chavane, Naaman, & Grinvald, 2004 in the context of the line-motion illusion. Applying sensitive dye optical imaging the authors showed that the spatiotemporal characteristic of sub-threshold cortical activity is consistent with the striking observation that non-moving stimuli can give rise to motion perception.

In the model we represent the paradigm of Experiment 2 by assuming that the horizontal positions of the comparison stimulus and the target stimulus are represented by two distinct local pools of neurons, P1 and P2, respectively. Each pool splits into an excitatory subpopulation  $u$  and an inhibitory subpopulation  $v$ , that is,  $P1 = (u1,v1)$  and  $P2 = (u2,v2)$ . As depicted in Fig. 6, the two pools are bilaterally coupled through sub-threshold spatial integration of activity (dashed lines). For simplicity we used scaled versions of the weight profiles shown in Fig. 5A for modelling the long-range connections between the four populations. Their standard deviations,  $\sigma_{sub,u}$  and  $\sigma_{sub,v}$ , determine the spatial extension of the horizontal spread of the sub-threshold activity. Excitation is mediated through direct connections whereas inhibitory input

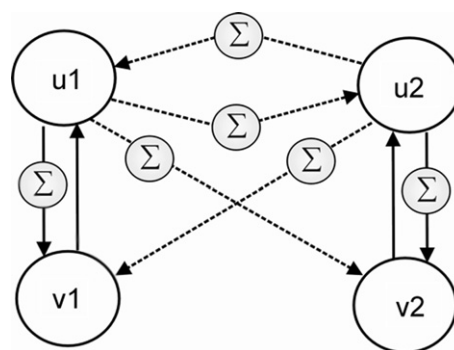


**Fig. 6.** Schematic view of the connectivity between the 4 subpopulations defining the model. Solid lines indicate the connections between the excitatory and the inhibitory subpopulations representing the same stimulus,  $(u1,v1)$  and  $(u2,v2)$ , respectively. An inhibitory neuron spatially integrates activity from excitatory neurons (as indicated by the summation sign) but feeds back only locally to the neuron with the same tuning properties. The dashed lines represent the long-range connections that mediate the integration of sub-threshold activity from an excitatory subpopulation encoding the horizontal position of the second stimulus.

comes through the inhibitory population that projects on the target neurons. The sub-threshold inhibition induced by the second stimulus thus appears to be delayed with respect to the sub-threshold excitation.

For the modelling we exploit the fact that there exists a threshold for triggering the self-stabilized population response of a local network. Weak input will only lead to a pre-activation of the target population. As we shall show, this pre-shaping may have nevertheless a significant effect on the time course and the position of the supra-threshold population response to an afferent input carrying retinal information.

To test our working hypothesis that the induced systematic changes in position may explain the relative localization errors we have to propose a mechanism how to read out the excitatory population responses encoding position. By taking the peak position as a read-out value we make the simplifying assumption that the shape of the activity distribution does not matter for the perceptual performance. For other paradigms like for instance discrimination tasks in which multiple stimuli have to be encoded by a single population this assumption may not be justified. It has been suggested that in this case an interpretation of the population response as a probability distribution over stimulus space may constitute a better predictor (Pouget, Dayan, & Zemel, 2000).

Since the internal representation is dynamic in space and time an obvious question concerns how to link the activity pattern to the single, unambiguous answer in the position judgment task. One possibility is that the visual system attributes the percept from a kind of snapshot at the point in time when a fixed internal criterion (e.g., an activation threshold) is reached. An alternative view postulates that the position information is computed by averaging over positions occupied by the population response in a small time window after the event (Eagleman, 2001). Here an additional process translates the spatial smear of peak positions into a single percept.

A discussion of the plausibility and neural implementation of different read-out mechanisms goes beyond the scope of this article. It is important, however, to stress that both proposed mechanisms could be used for the modelling. Appropriate choices of the parameter  $\Delta x$  controlling the drift and/or the time window for the temporal averaging will predict values for the localization judgment that are comparable with the predictions based on the snapshot mechanism.

Following our previous work we have chosen the peak position as a reference value for a comparison with the perceptual findings in the double stimulus paradigm. The internal criterion that

triggers the read-out process has been defined independently in a simulation that shall explain the absolute position error for a stimulus presented at 5°. The activation level at the time when the peak of the population response appears to be centred over 4.5° is taken as a fixed read-out threshold. The impact of the integration of sub-threshold input on the peak position can thus be compared relative to the order of magnitude of the displacement caused by the asymmetry in the recurrent interactions.

In Fig. 7 the response of the excitatory population to the comparison stimulus ( $u_1$ , solid line) and the target stimulus ( $u_2$ , dashed line) are shown at the time of the read-out for three differ-

ent SOAs. In each case the two stimuli were presented for 10 ms at position 5°. For the SOA of 150 ms (Fig. 7A), the afferent input carrying the information about the comparison stimulus interacts with a continuously growing sub-threshold activation level. As a result, the drift of the population response  $u_1$  in the direction of the fovea appears to be increased relative to the activity pattern representing  $u_2$ . The opposite is true for the SOA of 700 ms (Fig. 7C). Now the pre-shaping is suppressive leading to a substantial compensation of the drift induced by the asymmetric interactions. The amplitudes for the weight profiles describing the sub-threshold integration determine the relative strength of facilitation and suppression. The amplitude values have been chosen in the present simulations so that the transition from a positive to a negative relative localization error occurs at SOAs between 350 and 400 ms.

In Fig. 3 we depict the relative peak positions at a fixed activation level for all SOAs tested in the experiments (dashed line). A comparison shows that this measure explains qualitatively and quantitatively very well the experimental findings (solid line). Two additional points are worth mentioning. Since the sub-threshold interactions are equal for both populations, there is no relative mislocalization error when the stimuli are presented at the same time. However, the spread of sub-threshold excitation results in an absolute mislocalization error that exceeds the absolute error for a single stimulus by about 0.12°. For SOAs larger than 700 ms the suppressive effect of the sub-threshold interaction becomes continuously weaker and consequently the relative localization error decreases to zero.

While Experiment 2 addressed the temporal dimension of the interaction process, Experiment 3 investigated its spatial dimension. The findings showed that for a fixed SOA of 100 ms the magnitude of the relative error decreased with increasing vertical stimulus distance. In the model, the magnitude of the predicted error depends on the spatial extension of the sub-threshold activation of the excitatory population. The spread in horizontal direction is controlled by the spatial range of the sub-threshold integration modeled by the Gaussian weight profiles. To explain the experimental findings of Experiment 3 with our one-dimensional field model we have to make an additional assumption about the propagating of cortical sub-threshold activity which, however, seems plausible. We assume that a snapshot of the two-dimensional sub-threshold wave at a certain time after stimulus presentation (e.g., 100 ms) shows a horizontal spread of excitation that decreases with increasing vertical distance from the stimulated site. In numerical studies we systematically varied the standard deviations of the Gaussian weight profiles to simulate this assumed dependence on vertical distance. Expressed as multiples of the standard deviations,  $\sigma_{sub,u}$  and  $\sigma_{sub,v}$ , used to explain the findings of Experiment 3, the pairs  $(2\sigma_{sub,u}, 2\sigma_{sub,v})$ ,  $(\sigma_{sub,u}, \sigma_{sub,v})$  and  $(1/3\sigma_{sub,u}, 1/3\sigma_{sub,v})$  predict a relative localization error of 0.4°, 0.17° and 0.07°, respectively. These values are in good agreement with the values found in the experiments for the distances 0.7°, 2° and 6° (see Fig. 4). Since the spatial spread is proportional to  $\sigma_{sub,u}$  this result suggests that increasing the distance by a certain factor decreases the spread by roughly the same factor. In future work we plan to explicitly model the two-dimensional propagation of the sub-threshold activity.

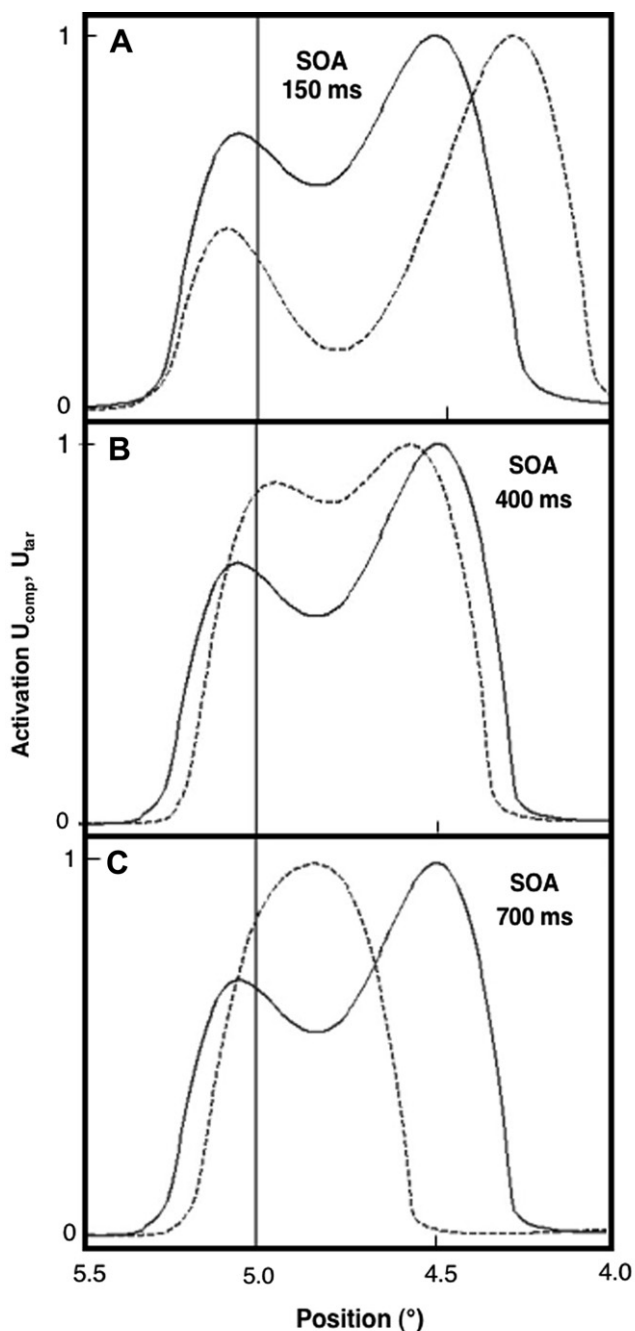


Fig. 7. In each of the three panels snapshots of the population activity associated with the target ( $u_{com}$ , dashed line) and the comparison stimulus ( $u_{tar}$ , solid line) are plotted. The snapshots are taken when the peak activity reaches a fixed read-out threshold. The two stimuli were presented with different SOAs: 150 ms (A), 400 ms (B), and 700 ms (C).

## Appendix A

In the following we describe in some detail the dynamic field model we used for simulating the processing of both the comparison and the target stimulus. Assuming that the number of excitatory and inhibitory neurons is large and that their receptive field centres densely cover the visual field, the mean activity at

time  $t$  of an excitatory neuron and an inhibitory neuron tuned to horizontal position  $x$  can be described by two continuous functions  $u(x,t)$  and  $v(x,t)$ , respectively. To model the dynamics of the neural populations we use the model class of neural fields first introduced and analyzed by Wilson and Cowan (1973). Neural field models are system-level models, which are adequate to describe the mean activity of large populations of neurons without referring to the detailed level of physiological realism. The temporal evolution of the activation variables ( $u_1, v_1$ ) and ( $u_2, v_2$ ) describing the four sub-populations is governed by the following system of coupled differential equations:

$$\begin{aligned} \tau \frac{d}{dt} u_1(x, t) &= -u_1(x, t) + h + S1(x, t) + \text{Sub}_{\text{ex},u_2}(x, t) + g(u_1(x, t)) \\ &\quad \left[ \int w_{uu}(x-x')f(u_1(x', t))dx' - v_1(x, t) \right] \\ \tau \frac{d}{dt} v_1(x, t) &= -v_1(x, t) + \text{Sub}_{\text{in},u_2}(x, t) + \int w_{uv}(x-x')f(u_1(x', t))dx' \\ \tau \frac{d}{dt} u_2(x, t) &= -u_2(x, t) + h + S2(x, t) + \text{Sub}_{\text{ex},u_1}(x, t) + g(u_2(x, t)) \\ &\quad \left[ \int w_{uu}(x-x')f(u_2(x', t))dx' - v_2(x, t) \right] \\ \tau \frac{d}{dt} v_2(x, t) &= -v_2(x, t) + \text{Sub}_{\text{in},u_1}(x, t) + \int w_{uv}(x-x')f(u_2(x', t))dx' \end{aligned}$$

The parameter  $\tau > 0$  is used to adjust the time scale of the field dynamics to the experimentally observed time scale. The constant  $h$  defines the resting level to which the population activity relaxes without external input. The integral terms describe the spatial summation of excitation in the two layers. The spatial interactions fall off with increasing distance between field sites:

$$W_{ui}(x-x') = A_i \exp\left(-\frac{(x-x')^2}{2\sigma_i^2}\right), \quad (i = u, v) \quad (\text{A.1})$$

where the choice of the relative amplitudes and spatial ranges,  $A_u > A_v$  and  $\sigma_u < \sigma_v$ , implements the Mexican-hat pattern. The weight profiles are shifted in “foveal” direction (see Fig. 5A) by an amount  $\Delta x$  which is chosen in the present simulations as 10% of  $\sigma_v$ .

Only sufficiently activated neurons contribute to the interaction. The nonlinear activation function  $f(u)$  is taken as a monotonic function of sigmoid shape going from 0 to 1:

$$f(u) = \frac{1}{1 + \exp(-\beta(u - u_f))} \quad (\text{A.2})$$

The parameter  $u_f$  determines the position of the maximum slope of the function  $f$ , and  $\beta$  controls the value of the maximum slope. The shunting function  $g(u)$  which is also of sigmoidal type (with parameters  $u_g$  and  $\beta$ ) does not play a functional role for the present application (but see Jancke et al., in press, for a discussion). The brief afferent inputs,  $S1(x,t)$  and  $S2(x,t)$ , to the excitatory populations are modelled as Gaussian profiles with space constant  $\sigma_s$  and amplitude  $A_s$ . The inputs were presented for 10 ms in all model simulations.

The terms

$$\text{Sub}_{\text{ex},ui}(x, t) = \int w_{\text{sub},u}(x-x')f(ui(x', t))dx' \quad \text{and}$$

$$\text{Sub}_{\text{in},ui}(x, t) = \int w_{\text{sub},v}(x-x')f(ui(x', t))dx', \quad i = 1, 2,$$

describe the summed sub-threshold input from the second excitatory population. The weight functions  $w_{\text{sub},u}(x,x')$  and  $w_{\text{sub},v}(x,x')$  are Gaussians with amplitudes  $A_{\text{sub},u}$ ,  $A_{\text{sub},v}$  and space constants  $\sigma_{\text{sub},u}$ ,  $\sigma_{\text{sub},v}$ , respectively. The amplitude values are adjusted to guarantee that this input alone does not trigger a supra-threshold population response.

For the model simulations a forward Euler integration scheme was used with a time step of 0.001 s, the fields consisted of 200 elements (spatial resolution: 10 elements = 0.1°). The numerical values for the model parameters describing the field interactions were within the range used in our previous work; they guarantee the existence of the localized transient activity pattern:  $\sigma_u = 0.15^\circ$ ,  $\sigma_v = 0.25^\circ$ ,  $A_u = 4.65$ ,  $A_v = 3.2$ ,  $\beta = 1$ ,  $u_f = u_g = 0$ ,  $h = -3$ .

The time scale of the field dynamics was  $\tau = 125$  ms, the parameters for the afferent input were  $\sigma_s = 0.15^\circ$  and  $A_s = 40$ , and the values describing the sub-threshold inputs were:  $A_{\text{sub},u} = 0.062$ ,  $A_{\text{sub},v} = 0.376$ ,  $\sigma_{\text{sub},u} = 0.15^\circ$ ,  $\sigma_{\text{sub},v} = 0.25^\circ$ .

## References

- Awatier, H., & Lappe, M. (2006). Mislocalization of perceived saccade target position induced by perisaccadic visual stimulation. *Journal of Neuroscience*, 26(1), 12–20.
- Berry, M. J., Brivanlou, I. H., Jordan, T. A., & Meister, M. (1999). Anticipation of moving stimuli by the retina. *Nature*, 398, 334–338.
- Brainard, D. H. (1997). The psychophysics toolbox. *Spatial Vision*, 10, 433–436.
- Brenner, E., Smeets, J. B. J., & van den Berg, A. V. (2001). Smooth eye movements and spatial localization. *Vision Research*, 41, 2253–2259.
- Eagleman, D. M. (2001). Visual illusions and neurobiology. *Nature Reviews*, 2, 920–926.
- Erlhagen, W. (2003). Internal models for visual perception. *Biological Cybernetics*, 88, 409–417.
- Erlhagen, W., & Jancke, D. (2004). The role of action plans and other cognitive factors in motion extrapolation: A modelling study. *Visual Cognition*, 11(2/3), 315–340.
- Fahle, M. (1991). Psychophysical measurements of eye drifts and tremor by dichoptic or monocular vernier acuity. *Vision Research*, 31, 209–222.
- Findlay, J. M. (1974). Direction perception and human fixation eye movements. *Vision Research*, 14, 703–711.
- Fitzpatrick, D. (2000). Seeing beyond the receptive field in primary visual cortex. *Current Opinion in Neurobiology*, 10, 438–443.
- Foley, J. M. (1976). Successive stereo and vernier position discrimination as a function of dark interval. *Vision Research*, 16, 1269–1273.
- Hagenaar, R., & van der Heijden, A. H. C. (1997). On the relation between type of arrays and type of errors in partial-report bar-probe studies. *Acta Psychologica*, 88, 89–104.
- Huynh, H., & Feldt, L. S. (1980). Performance of traditional  $F$ -test in repeated measure designs under covariance heterogeneity. *Communication in Statistics: Theory and Methods*, A9, 61–74.
- Jancke, D., & Erlhagen, W. (in press). Bridging the gap: A model of common neural mechanisms underlying the Fröhlich effect, the flash-lag effect, and the representational momentum effect. In R. Nijhawan & B. Khurana (eds.), *Space and time in perception and action*. Cambridge, UK: Cambridge University Press.
- Jancke, D., Chavane, F., Naaman, S., & Grinvald, A. (2004). Imaging correlates of visual illusion in early visual cortex. *Nature*, 428, 423–426.
- Jancke, D., Erlhagen, W., Dinse, H. R., Akhavan, A. C., Giese, M., Steinhage, A., et al. (1999). Parametric population representation of retinal location: Neuronal interaction dynamics in cat primary visual cortex. *Journal of Neuroscience*, 19, 9016–9028.
- Kerzel, D. (2002). Memory for the position of stationary objects: Disentangling foveal bias and memory averaging. *Vision Research*, 42(2), 159–167.
- Kirschfeld, K., & Kammer, T. (1999). The Fröhlich effect: A consequence of the interaction of visual focal attention and metacontrast. *Vision Research*, 39(22), 3702–3709.
- Klein, R. M. (2000). Inhibition of return. *Trends in Cognitive Sciences*, 4(4), 138–147.
- Matin, L., Pola, J., Matin, E., & Picoult, E. (1981). Vernier discrimination with sequentially flashed lines: Roles of eye movements retinal offsets and short-term memory. *Vision Research*, 21, 556–647.
- Müsseler, J., & Aschersleben, G. (1998). Localising the first position of a moving stimulus: The Fröhlich Effect and an attention-shifting explanation. *Perception & Psychophysics*, 60, 683–695.
- Müsseler, J., Stork, S., & Kerzel, D. (2002). Comparing mislocalizations in movement direction: The Fröhlich effect, the flash-lag effect and the representational momentum. *Visual Cognition*, 9, 120–138.
- Müsseler, J., & van der Heijden, A. H. C. (2004). Two spatial maps contributing to perceived space: Evidence from a relative mislocalization. *Visual Cognition*, 11(2/3), 235–254.
- Müsseler, J., van der Heijden, A. H. C., Mahmud, S. H., Deubel, H., & Ertsey, S. (1999). Relative mislocalization of briefly presented stimuli in the retinal periphery. *Perception & Psychophysics*, 61(8), 1646–1661.
- O'Regan, J. K. (1984). Retinal versus extraretinal influences in flash localization during saccadic eye movements in the presence of a visible background. *Perception and Psychophysics*, 36, 1–14.
- Pelli, D. G. (1997). The VideoToolbox software for visual psychophysics: Transforming numbers into movies. *Spatial Vision*, 10, 437–442.
- Posner, I. M., & Cohen, Y. (1984). Components of visual orienting. In H. Bouma & D. G. Bouwhuis (Eds.), *Attention and performance X* (pp. 531–556). Hillsdale, NJ: Lawrence Erlbaum.

- Pouget, A., Dayan, P., & Zemel, R. (2000). Information processing with population codes. *Nature Reviews*, 1, 125–132.
- Rotman, G., Brenner, E., & Smeets, J. B. J. (2005). Flashes are localized as if they were moving with the eyes. *Vision Research*, 45, 355–364.
- Sheth, B. R., & Shimojo, S. (2001). Compression of space in visual memory. *Vision Research*, 41(3), 329–341.
- Uddin, M. K., Kawabe, T., & Nakamizo, S. (2005). Differential roles of distracters in reflexive and memory-based localization. *Spatial Vision*, 18, 579–592.
- van der Heijden, A. H. C., Müsseler, J., & Bridgeman, B. (1999a). On the perception of position. In G. Aschersleben, T. Bachmann, & J. Müsseler (Eds.), *Cognitive contribution to the perception of spatial and temporal events* (pp. 19–38). North-Holland: Elsevier.
- van der Heijden, A. H. C., van der Geest, J. N., De Leeuw, F., Krikke, K., & Müsseler, J. (1999b). Sources of position-perception error for small isolated targets. *Psychological Research*, 62, 20–35.
- Wichmann, F. A., & Hill, N. J. (2001a). The psychometric function: I. Fitting, sampling, and goodness of fit. *Perception & Psychophysics*, 63, 1293–1313.
- Wichmann, F. A., & Hill, N. J. (2001b). The psychometric function: II. Bootstrap-based confidence intervals and sampling. *Perception & Psychophysics*, 63, 1314–1329.
- Wilson, H. R., & Cowan, J. D. (1973). A mathematical theory of the functional dynamics of cortical and thalamic nervous tissue. *Kybernetik (Biological Cybernetics)*, 13, 55–80.